

The “Topography” of Glaucomatous Defect Using OCT and Visual Field Examination

Alessandro de Paula¹ , Andrea Perdicchi², Augusto Pocobelli³, Serena Fragiotta⁴, Gianluca Scuderi⁵

ABSTRACT

Aim: To describe the modifications in the superior and inferior retinal nerve fiber layer (RNFL) thickness regarding the distribution of the VF defects for the horizontal meridians in glaucomatous patients and the differences in the RNFL thickness topography between glaucomatous and healthy subjects.

Methods: One hundred twenty eyes of 91 patients affected by glaucoma and 94 eyes of 51 normal patients were retrospectively reviewed. Computerized 30°VF (Octopus G1 Dynamic strategy) and optical coherence tomography (OCT) ONH and 3D disk analysis were performed in all cases. The RNFL thickness measures analyzed in both groups were superior-nasal (SN), superior-temporal (ST), inferior-nasal (IN), and inferior temporal (IT) sectors. The VFs were classified according to the distribution of the VF defect as for the horizontal meridian in the pattern deviation plot as superior, inferior, predominantly superior, or predominantly inferior.

Result: In the glaucomatous group, 78 eyes (65%) showed a predominantly superior VF defect, while 38 eyes (32%) showed a predominantly inferior VF defect. Fifty-six eyes (46.7%) presented an exclusively superior, and 27/120 eyes (22.5%) presented an exclusively inferior VF defect. In the control group, the thickest RNFL sector was IT. The ST sector showed the thickest RNFL in presence of an exclusive superior VF defect. In case of an exclusive inferior VF defect, the thickest RNFL was the IT sector. VF showing superior defect presented a more altered MD than the VF with an inferior defect.

Conclusion: Glaucomatous damage affects both the superior and inferior neural rim almost simultaneously. However, the neural rim loss seems to be asymmetric, involving the inferior or superior rim depending on the predominant involvement of the superior or inferior hemifield at the VF test. Particularly, the IT sector appears to be the most compromised in glaucomatous eyes. Therefore, the asymmetry between superior and inferior RNFL could support the diagnosis of glaucoma.

Keywords: Glaucoma, OCT, RNFL, Visual field.

Journal of Current Glaucoma Practice (2022): 10.5005/jp-journals-10078-1353

INTRODUCTION

Glaucomatous disease is a degenerative optic neuropathy leading to apoptosis of retinal ganglion cells and cupping of the optic nerve head.¹ It leads to a progressive alteration of the visual field (VF).² Therefore, the computerized VF test has become the gold standard for detecting the onset and the evolution of glaucomatous defects.^{3,4} The retinal fiber layer (RNFL) and the ganglion cell complex (GCC) analysis obtained through optical coherence tomography (OCT) demonstrated a good correlation with retinal sensitivity detected on the VF test,⁵⁻⁷ even at the pre-perimetric stage.⁸

Several risk factors have been involved in developing glaucoma, including older age, increased cup-disk ratio, high intraocular pressure (IOP), a higher pattern standard deviation, and thinner central corneal thickness.⁹ Nevertheless, IOP reduction is still considered the most relevant therapeutic approach to prevent further glaucomatous damage.¹⁰⁻¹³ The optic nerve head morphology is pivotal to diagnose the disease. When estimating the optic disk, the presence of vertical cupping is highly indicative of glaucomatous damage.^{9,14}

The present study aimed to describe the modifications in the thickness of superior and inferior peripapillary nerve fibers regarding the distribution of the VF defects for the horizontal meridians in POAG patients and the possible clinical implications related to a predominantly superior or inferior VF defect among glaucomatous eyes. Moreover, to reveal possible differences in the peripapillary nerve fiber topography between glaucomatous and healthy subjects.

^{1,3}Department of Head-neck, San Giovanni Addolorata Hospital, Uoc Oftalmologia - Banca Degli Occhi, Rome, Italy

^{2,4,5}Department of NESMOS, St. Andrea Hospital, University of Rome La Sapienza, Rome, Italy

Corresponding Author: Alessandro de Paula, Department of Head-neck, San Giovanni Addolorata Hospital, Uoc Oftalmologia - Banca Degli Occhi, Rome, Italy, Phone: +39 0677052950, e-mail: aledepaula@hotmail.it

How to cite this article: de Paula A, Perdicchi A, Pocobelli A, *et al.* The “Topography” of Glaucomatous Defect Using OCT and Visual Field Examination. *J Curr Glaucoma Pract* 2022;16(1):31–35.

Source of support: Nil

Conflicts of Interest: None

MATERIALS AND METHODS

Two hundred fourteen eyes of 142 Caucasian patients were retrospectively reviewed. Of these, 120 eyes of 91 patients (70.88 ± 10.54 years) suffering from glaucoma, while 94 eyes of 51 patients (56.96 ± 13.47 years) served as controls. The study complied with the tenets of the Declaration of Helsinki and with the Health Insurance Portability and Accountability Act of 1996.

POAG patients were defined as: untreated IOP > 21 mm Hg, glaucomatous features of optic nerve head, identifiable trabecular meshwork at gonioscopy, at least three adjacent points with a level of significance inferior to 5% on the pattern deviation plot with at least 1 point with a significance inferior to 1% at visual

field examination, or an abnormal glaucoma hemifield test, or a loss variance (LV) <2.5 dB, and one or more abnormal RNFL sectors at spectral-domain (SD) OCT exam. The control group consisted of subjects with an unremarkable ophthalmic examination and ophthalmoscopically normal optic nerve head appearance, IOP inferior to 21 mm Hg, absence of visual field defects on Octopus visual field test (Octopus G1 Dynamic strategy), and RNFL sectors within normal limits at SD-OCT. Exclusion criteria were: spherical defect greater than ± 5 diopters, ocular media opacities that preclude the execution of VF or OCT, any other ocular pathologies, retinal laser photocoagulation, or previous ocular surgery other than trabeculectomy or phacoemulsification of cataract.

OCT Examination

All subjects were analyzed on SD-OCT (iVue Optovue Inc., Fremont, CA) using ONH and 3D disk analysis. Scans with quality/signal strength inferior to 40/100 were not considered suitable for the study.

The software automatically generates a map showing the RNFL thickness measured 3.45-mm from the center of the optic disk. The RNFL thickness measures analyzed in both groups were superior-nasal (SN), superior-temporal (ST), inferior-nasal (IN), and inferior temporal (IT) sectors (Fig. 1).

Visual Field Assessment

Computerized 30°VF using Octopus G1 Dynamic strategy was performed in all cases. The VF exams with false-negative errors greater than 15%, false-positive errors greater than 15%, and fixation loss > 20% were excluded. The VFs were grouped

according to the distribution of the VF defect as for the horizontal meridian in the pattern deviation plot as superior or inferior. The VFs were predominantly superior or predominantly inferior when more than 50% of the defects were located in the respective hemifield.

Statistical Analysis

Parameters are expressed as mean ± standard deviation. *t*-test was used to establish the statistical significance of differences between variables. *p* values less than 0.05 were considered statistically significant. SPSS software (ver.20; SPSS, Inc., Chicago, IL) was used for statistics.

RESULTS

The average mean defect was -9.61 ± 5.68 dB (ranging from -0.7 to -26.3 dB) in the glaucomatous group and +0.14 ± 1.5 dB in the control group (ranging from +3.4 to -4.3 dB, *p*.0001). In the glaucomatous group, 78 eyes (65%) showed a predominantly superior VF defect, while 38 eyes (32%) showed a predominantly inferior VF defect, and four eyes (3%) did not exhibit any predominant hemifield distribution. Moreover, 56/120 eyes (46.7%) presented an exclusively superior, and 27/120 eyes (22.5%) presented an exclusively inferior VF defect.

In the control group, the thickest RNFL sector was IT, followed by ST, IN, and SN sectors (Table 1). However, in the glaucomatous group, the ST represented the thickest RNFL sector with no statistical differences among the other sectors (*p*>0.05) (Table 1). Of note, the ST remained the thickest sector even in eyes with an exclusive superior defect at VF examination; no significant differences

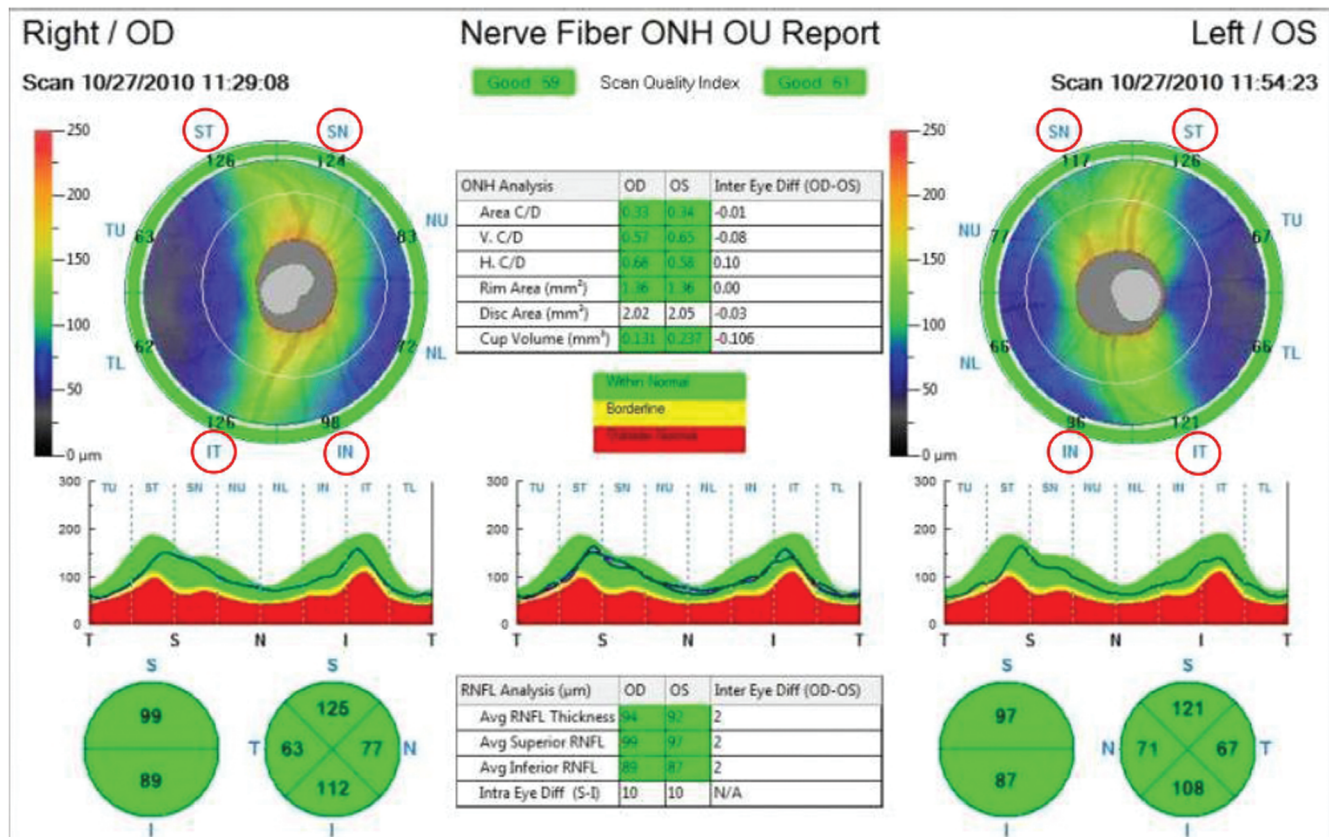


Fig. 1: OCT ONH analysis showing the analyzed sectors



were appreciated between the inferior sectors (IN and IT) in this subgroup (Table 1).

Eyes with an exclusive inferior VF defect demonstrated the thickest RNFL in the IT sector, followed by ST, IN, and SN sectors. However, no statistical difference was appreciated between the ST and IN sectors thickness ($p > 0.05$) in this group (Table 1). When analyzing the nerve fibers in the corresponding sectors, the inferior sectors (IT and IN) resulted thicker than the corresponding superior sectors either in the control group (ST vs IT 130.28 μm vs 133.48 μm , $p = 0.016$; SN vs IN 100.68 μm vs 106.6 μm , $p = 0.003$) and in the subgroups with a pure inferior VF defect (ST vs IT 83.26 vs 91.48, $p = 0.013$; SN vs IN 76.59 μm vs 81.96 μm , $p = 0.049$).

On the contrary, the RNFL in the ST sector was thicker than the IT one in the glaucomatous group (ST vs IT 90.8 μm vs 77.1 μm , $p < 0.0001$) and in the solely superior defect group (ST vs IT 98.02 vs 74.27, $p > 0.0001$) (Table 2).

By comparing subgroups with VF defects localized in a given hemifield, the superior VF defect presented a more altered MD than the inferior VF defect group (-8.91 vs -5.62, $p = 0.0007$). However, the groups were comparable regarding IOP (16.41 \pm 4.29 mm Hg vs 15.93 \pm 2.66 mm Hg, $p = 0.27$) and age (71.11 \pm 9.57 years vs 70.4 \pm 9 years .31).

Eyes with a VF defect limited to a single hemifield demonstrated a reduction of the RNFL sectors also in correspondence of the unaffected hemifield, the magnitude of reduction was 24.76% for the ST sector, 19.68% for the SN sector, 31.46% for the IT sector, and 23.15% for the IN sector compared to controls.

Conversely, the RNFL sector corresponding to abnormal hemifield showed a reduction of 36.10%, 24%, 44.38%, and 28.66%, for ST, SN, IT, and IN sectors compared to controls.

DISCUSSION

In glaucomatous eyes, the VF defects above the horizontal meridian occur more commonly than those below the horizontal meridian, as previously described.¹⁵⁻¹⁸ Our results corroborated that the superior VF defect was the most represented in glaucomatous eyes with 65% of cases. Interestingly, the thickest RNFL sector represented by the IT in normal subjects was instead the thinnest sector in glaucomatous eyes, indicating its high susceptibility to glaucomatous damage.

Similar results on the topographical distribution of the RNFL glaucomatous damage have been reported by Leung et al.¹⁹ and Jonas et al.²⁰ A recent study conducted by OCT angiography suggested an IOP-related effect on capillary density interesting the inferior sectors preferentially.²¹ Likewise, Leung et al.²² described that the RNFL defects in glaucoma most frequently affected IT followed by the ST sectors. Our findings further confirmed the existing literature and demonstrated that this peculiar sectorial RNFL involvement is maintained in patients with localized superior and inferior VF defects.

Although the glaucomatous damage involves the neural rim diffusely, the asymmetric VF depression presented an anatomical correspondence with the RNFL defects. The altered superior VF affected the inferior rim and vice versa. The relationship between the inferior RNFL thinning and the superior hemifield defect at the VF and between the superior RNFL sectors and the inferior hemifield

Table 1: RNFL thickness in each sector for each group

| Control group | Glaucoma group | Superior defect group | Inferior defect group |
|--|---|---|---|
| IT (133.48 \pm 13.93 μm) | ST (90.08 \pm 22.04 μm) | ST (98.02 \pm 25.97 μm) | IT (91.48 \pm 19.34 μm) |
| ST (130.28 \pm 13 μm) | SN (77.64 \pm 17.34 μm) | SN (80.95 \pm 18.81 μm) | ST (83.26 \pm 14.66 μm) |
| IN (106.65 \pm 19.82 μm) | IT (77.1 \pm 18.16 μm) | IN (75.43 \pm 23.20 μm) | IN (81.96 \pm 14.66 μm) |
| SN (100.68 \pm 12.16 μm) | IN (75.3 \pm 19.1 μm) | IT (74.27 \pm 16.34 μm) | SN (76.59 \pm 14.70 μm) |

ST, superior-temporal sector; IT, inferior-temporal sector; SN, superior-nasal sector; IN, inferior-nasal sector. There is no difference ($p > 0.05$) between the values in bold in each group

Table 2: Comparison between RNFL thicknesses of each sector

| | Control group | Glaucoma group | Superior defect group | Inferior defect group |
|----------|--|---|--|---|
| ST vs IT | 130.28 \pm 13 vs 133.48 \pm 13.93 ($p = 0.016$) | 90.8 \pm 22.04 vs 77.1 \pm 18.16 ($p < 0.0001$) | 98.02 \pm 25.97 vs 74.27 \pm 16.34 ($p < 0.0001$) | 83.26 \pm 14.66 vs 91.48 \pm 19.34 ($p = 0.013$) |
| SN vs IN | 100.78 \pm 12.6 vs 106.65 \pm 19.82 ($p = 0.003$) | 77.64 \pm 17.34 vs 75.3 \pm 19.1 ($p = 0.086$) | 80.95 \pm 18.81 vs 75.43 \pm 23.20 ($p = 0.022$) | 76.59 \pm 14.7 vs 81.96 \pm 14.66 ($p = 0.049$) |
| ST vs SN | 130.28 \pm 13 vs 100.78 \pm 12.6 ($p < 0.0001$) | 90.8 \pm 22.04 vs 77.64 \pm 17.34 ($p < 0.0001$) | 98.02 \pm 25.97 vs 80.95 \pm 18.81 ($p.0001$) | 83.26 \pm 14.66 vs 76.59 \pm 14.7 ($p = 0.009$) |
| IT vs IN | 133.48 \pm 13.93 vs 106.65 \pm 19.82 ($p.0001$) | 77.1 \pm 18.16 vs 75.3 \pm 19.1 ($p = 0.11$) | 74.27 \pm 16.34 vs 75.43 \pm 23.20 ($p = 0.31$) | 91.48 \pm 19.36 vs 81.96 \pm 14.66 ($p = 0.003$) |
| ST vs IN | 130.28 \pm 13 vs 106.65 \pm 19.82 ($p.0001$) | 90.08 \pm 22.04 vs 75.3 \pm 19.1 ($p.001$) | 98.02 \pm 25.97 vs 75.43 \pm 23.20 ($p.0001$) | 83.26 \pm 14.66 vs 81.96 \pm 14.66 ($p = 0.34$) |
| SN vs IT | 100.78 \pm 12.16 vs 133.48 \pm 13.93 ($p.0001$) | 77.64 \pm 17.34 vs 77.1 \pm 18.16 ($p = 0.38$) | 80.95 \pm 18.81 vs 74.27 \pm 16.34 ($p = 0.007$) | 76.59 \pm 14.7 vs 91.48 \pm 19.34 ($p.0001$) |

ST, Superior-temporal sector; IT, Inferior-temporal sector; SN, Superior-nasal sector; IN, Inferior-nasal sector

was recently described also by Sánchez-Pulgarín et al.²³ In our series, the analysis of glaucomatous eyes with a mere superior or inferior hemifield defect further confirmed such previous findings.

Another interesting finding regards the evidence of a worse MD in eyes with a superior defect at the VF despite the similar IOP values and age with eyes with an inferior defect. In a previous retrospective study, it has been demonstrated that the VF defects located in the superior hemifields tend to progress faster than those located inferiorly.²⁴ Similarly, the macular ganglion cell-inner plexiform layer follows the same trend of progression.²⁵

Our findings indicate that when one hemifield at the VF is affected, the RNFL corresponding to the normal hemifield was also reduced compared to the control group. A possible explanation is represented by the evidence that the morphological damage of the optic nerve precedes the perimetric alteration.²⁶ Bartz-Schmidt reported that at least 40% of the neural rim is lost before the occurrence of VF damage.²⁷ The study specified that VF defects become detectable after an RNFL loss of 24.7–36.1% for the ST sector, between 19.7 and 24% for the SN sector, 31.5–44.4% for the IT, and between 23.15% and 28.66% for the IN sector. Perhaps the greatest thickness of the IT sector in normal eyes may represent the reason for the need for a more profound RNFL loss before a VF defect becomes detectable.

Despite its retrospective nature, this study confirmed the relevance of the asymmetry when considering the RNFL thickness evaluation between the ST and IT sectors, particularly when comparing glaucomatous with normal subjects.

In conclusion, glaucomatous damage affects both the superior and inferior neural rim almost simultaneously. However, the neural rim loss seems to be asymmetric, involving the inferior or superior rim depending on the predominant involvement of the superior or inferior hemifield at the VF test. Particularly, the IT sector appears to be the most compromised in glaucomatous eyes. Therefore, the asymmetry between superior and inferior RNFL could support the diagnosis of glaucoma. Furthermore, this study confirmed that the superior VF defect, although more frequent, exhibited a worse functional prognosis compared to inferior involvement.

ORCID

Alessandro De Paula  <https://orcid.org/0000-0002-9738-4789>

REFERENCES

- Scuderi G, Khaw PT, Medeiros FA, et al. Challenging laucomas: update on diagnosis and management. *J Ophthalmol* 2016;6935086. DOI: 10.1155/2016/6935086
- Shon K, Wollstein G, Schuman JS, et al. Prediction of glaucomatous visual field progression: pointwise analysis. *Curr Eye Res* 2014;39(7):705–710. DOI: 10.3109/02713683.2013.867353
- Scuderi GL, Cesareo M, Perdicchi A, et al. Standard automated perimetry and algorithms for monitoring glaucoma progression. *Prog Brain Res* 2008;173:77–99. DOI: 10.1016/s0079-6123(08)01107-2
- Perdicchi A, Abdolrahimzadeh S, Cutini A, et al. Evaluation of the progression of visual field damage in patients suffering from early manifest glaucoma. *Clin Ophthalmol* 2016;25(10):1647–1651. DOI: 10.2147/OPHTH.S113995
- Shin HY, Park HY, Jung KI, et al. Comparative study of macular ganglion cell-inner plexiform layer and peripapillary retinal nerve fiber layer measurement: structure-function analysis. *Invest Ophthalmol Vis Sci* 2013;54(12):7344–7353. DOI: 10.1167/iovs.13-12667
- Leung CK, Chan WM, Chong KK, et al. Comparative study of retinal nerve fiber layer measurement by stratusOCT and GDx VCC, I: correlation analysis in glaucoma. *Invest Ophthalmol Vis Sci* 2005;46(9):3214–3220. DOI: 10.1167/iovs.05-0294
- Scuderi G, Fragiotta S, Scuderi L, et al. Ganglion cell complex analysis in glaucoma patients: what can it tell us? *Eye Brain* 2020;12:33–44. DOI: 10.2147/EB.S226319
- Perdicchi A, de Paula A, Sordi E, et al. Cluster analysis of computerized visual field and optical coherence tomography-ganglion cell complex defects in high intraocular pressure patients or early-stage glaucoma. *Eur J Ophthalmol* 2020;30(3):475–479. DOI: 10.1177/1120672119841774
- Gordon MO, Beiser JA, Brandt JD, et al. The ocular hypertension treatment study: baseline factors that predict the onset of primary open-angle glaucoma. *Arch Ophthalmol* 2002;120(6):714–720. DOI: 10.1001/archophth.120.6.714
- The advanced glaucoma intervention study (AGIS): 7. the relationship between control of intraocular pressure and visual field deterioration. *Am J Ophthalmol* 2000;130(4):429–440. DOI: 10.1016/s0002-9394(00)00538-9
- Leske MC, Heijl A, Hussein M, et al. Factors for glaucoma progression and the effect of treatment: the early manifest glaucoma trial. *Arch Ophthalmol* 2003;121(1):48–56. DOI: 10.1001/archophth.121.1.48
- Kass MA, Heuer DK, Higginbotham EJ, et al. The ocular hypertension treatment study: a randomized trial determines that topical ocular hypotensive medication delays or prevents the onset of primary open-angle glaucoma. *Arch Ophthalmol* 2002;120(6):701–713. DOI: 10.1001/archophth.120.6.701
- Miglior S, Zeyen T, Pfeiffer N, et al. European glaucoma prevention study: author reply. *Ophthalmology* 2005;112(3):366–375. DOI: 10.1016/j.ophtha.2004.11.030
- Quigley HA, Green WR. The histology of human glaucoma cupping and optic nerve damage: clinicopathologic correlation in 21 eyes. *Ophthalmology* 2020;127(4S):S45–S69. DOI: 10.1016/j.ophtha.2020.01.035
- Heijl A, Lundqvist L. The frequency distribution of earliest glaucomatous visual field defects documented by automatic perimetry. *Acta Ophthalmol (Copenh)* 1984;62(4):658–664. DOI: 10.1111/j.1755-3768.1984.tb03979.x
- Hart WM, Becker B. The onset and evolution of glaucomatous visual field defects. *Ophthalmology* 1982;89(3):268–279. DOI: 10.1016/s0161-6420(82)34798-3
- Drance SM. The glaucomatous visual field. *Br J Ophthalmol* 1972;56(3):186–200. DOI: 10.1136/bjo.56.3.186
- Lan YW, Henson DB, Kwartz AJ. The correlation between optic nerve head topographic measurements, peripapillary nerve fibre layer thickness, and visual field indices in glaucoma. *Br J Ophthalmol* 2003;87(9):1135–1141. DOI: 10.1136/bjo.87.9.1135
- Leung CK, Yu M, Weinreb RN, et al. Retinal nerve fiber layer imaging with spectral-domain optical coherence tomography: patterns of retinal nerve fiber layer progression. *Ophthalmology* 2012;119(9):1858–1866. DOI: 10.1016/j.ophtha.2012.03.044
- Jonas JB, Fernandez MC, Sturmer J. Pattern of glaucomatous neuroretinal rim loss. *Ophthalmology* 1993;100(1):63–68. DOI: 10.1016/s0161-6420(13)31694-7
- Paula A, Perdicchi A, Tizio FD, et al. Effect of intraocular pressure lowering on the capillary density of optic nerve head and retinal nerve fiber layer in patients with glaucoma. *Eur J Ophthalmol* 2021;31(6):3003–3009. DOI: 10.1177/1120672120967233
- Leung CK, Choi N, Weinreb RN, et al. Retinal nerve fiber layer imaging with spectral-domain optical coherence tomography: pattern of RNFL defects in glaucoma. *Ophthalmology* 2010;117(12):2337–2344. DOI: 10.1016/j.ophtha.2010.04.002
- Sanchez-Pulgarín M, Saenz-Frances F, Martínez-de-la-Casa JM, et al. Structure-function relationship in a series of glaucoma cases. *J Fr Ophthalmol* 2020;43(2):111–122.
- Cho HK, Kee C. Comparison of the progression rates of the superior, inferior, and both hemifield defects in normal-tension glaucoma patients. *Am J Ophthalmol* 2012;154(6):958–968.e1. DOI: 10.1016/j.ajo.2012.05.025



25. Choi JA, Shin HY, Park HL, et al. The pattern of retinal nerve fiber layer and macular ganglion cell-inner plexiform layer thickness changes in glaucoma. *J Ophthalmol* 2017;2017:6078365. DOI: 10.1155/2017/6078365
26. Johnson CA, Adams AJ, Casson EJ, et al. Blue-on-yellow perimetry can predict the development of glaucomatous visual field loss. *Arch Ophthalmol* 1993;111(5):645–650. DOI: 10.1001/archopht.1993.01090050079034
27. Bartz-Schmidt KU, Thumann G, Jonescu-Cuypers CP, et al. Quantitative morphologic and functional evaluation of the optic nerve head in chronic open-angle glaucoma. *Surv Ophthalmol* 1999;44 Suppl 1: S41–53. DOI: 10.1016/s0039-6257(99)00076-4